Supplementary Materials

A hierarchical lectin-based multimodal workflow for spatial mapping of extracellular matrix glycans in fibrotic hearts

Patcharaporn Boottanun[1,2], Chiaki Nagai-Okatani[1]*, Kunio Kawanishi[3,4], Masaki Baba[3,5], Tomofumi Nakatsukasa[6], Tomoko Ishizu[6], Kiyohiko Angata[1,2], Atsushi Kuno[1]

[1] Cellular and Molecular Biotechnology Research Institute, National Institute of Advanced Industrial Science and Technology, Japan

[2] Glycan and Life Systems Integration Center (GaLSIC), Soka University, Japan

[3] Department of Anatomy, Showa Medical University School of Medicine, Japan

[4] Department of Experimental Pathology, Institute of Medicine, University of Tsukuba, Japan

[5] Department of Diagnostic Pathology, Institute of Medicine, University of Tsukuba, Japan

[6] Department of Cardiology, Institute of Medicine, University of Tsukuba, Japan

* Correspondence: C. Nagai-Okatani (e-mail: chiaki-okatani@aist.go.jp).

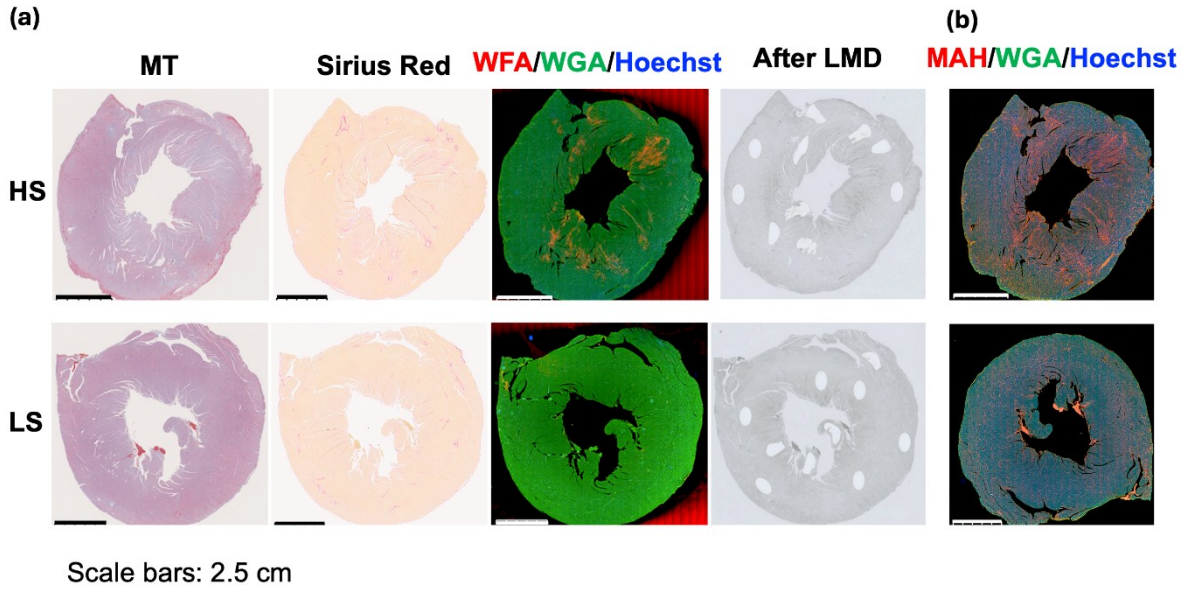

Supplementary Fig. 1 Representative whole-section images for tissue collection using laser microdissection (LMD) (a) and *Maackia amurensis* hemagglutinin (MAH) staining (b). Fibrotic areas were determined based on collagen staining with Masson's trichrome (MT) and Sirius red, where *Wisteria floribunda* agglutinin (WFA) staining was positive. The WFA staining patterns were used to determine the collection areas for LMD. The staining sections and the section after LMD are shown for representative high-salt-treated (HS) and low-salt-treated (LS) rats. MAH staining was performed to validate the fibrosis-associated glycan signals identified by tissue glycome mapping. Wheat germ agglutinin (WGA) and Hoechst were used for staining the membrane and nucleus, respectively.

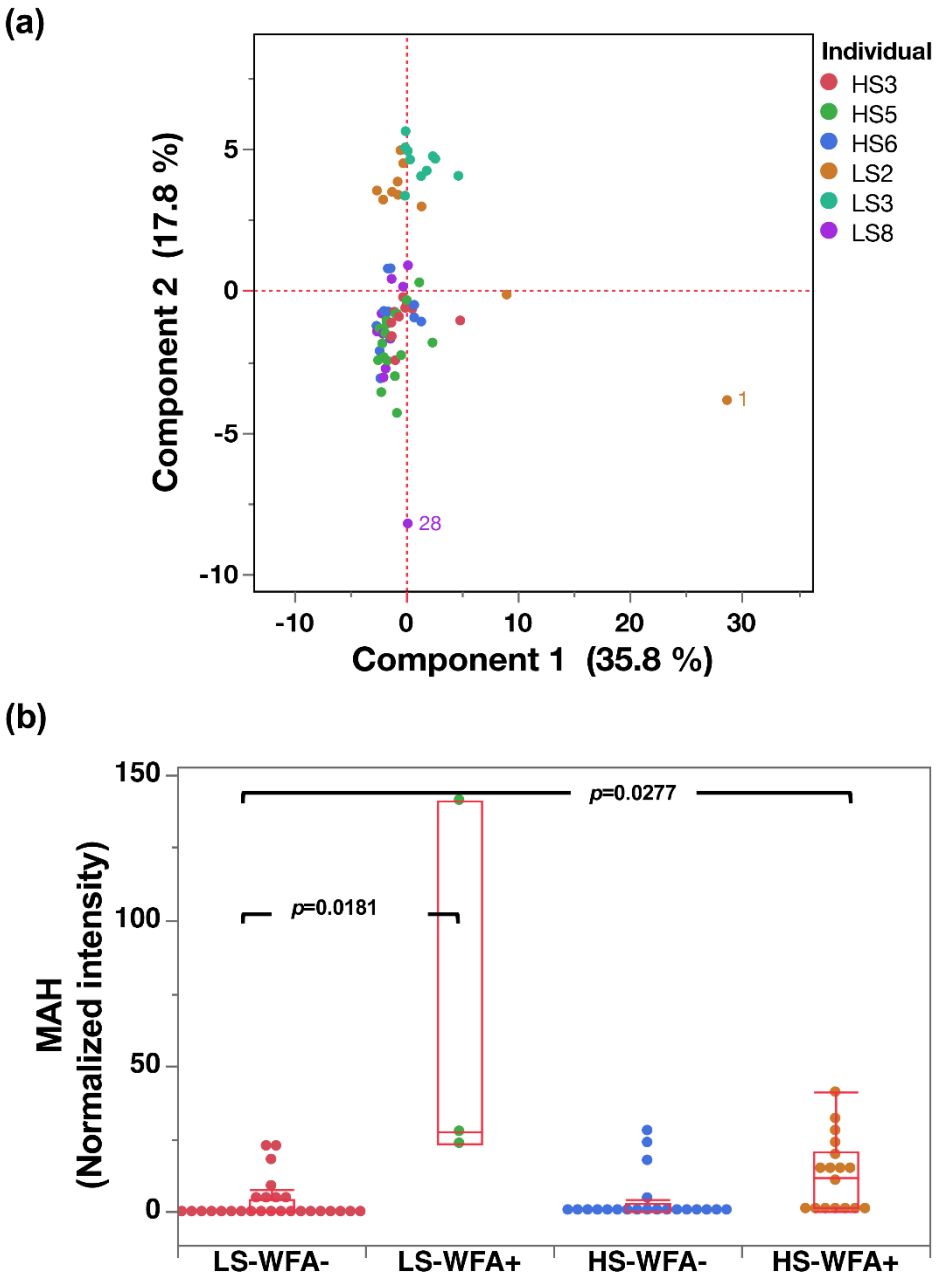

Supplementary Fig. 2 The normalized intensities of glycomic profiles obtained from HS and LS heart samples at the same exposure time were assessed using principal component analysis (PCA). PCA was used as an exploration tool to assess the main sources of variance (a). Since the glycomic profiles of some samples differed significantly according to differences likely attributable to experimental batch variation, LS2 and LS3 were subjected to sensitivity analyses rather than exclusion. The PCA after excluding LS2 and LS3 is shown in main text **Fig. 1c**. The statistical analysis including LS2 and LS3 samples was also performed (b), and the result showed that the exclusion of these samples did not alter the main conclusions that MAH-reactive glycans were increased in WFA-positive (WFA^+) areas.

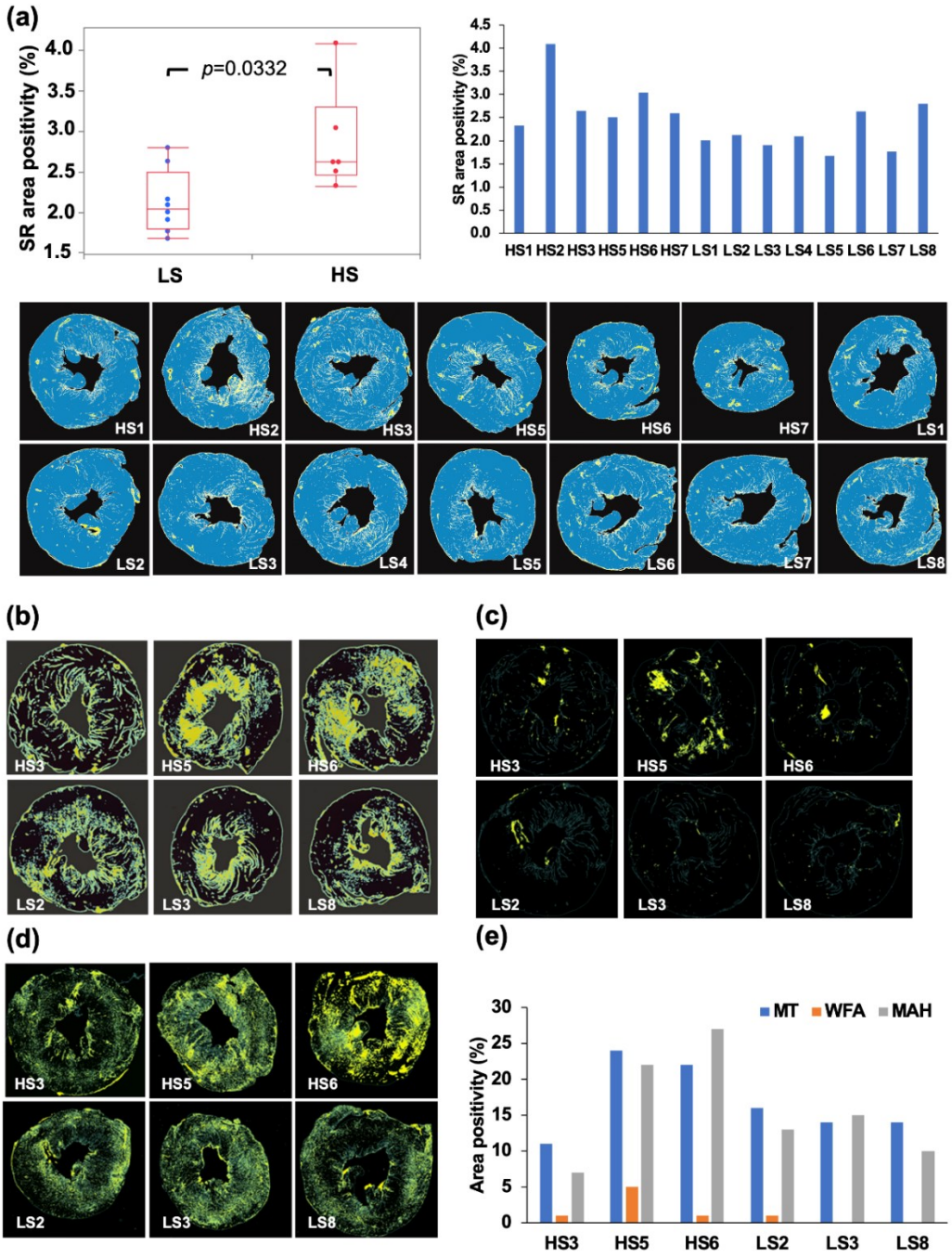

Supplementary Fig. 3 Comparison between collagen deposition and aberrant glycosylation. The proportion of Sirius Red $(SR)^{+}$ fibrotic areas relative to the total tissue area were compared between HS and LS tissues (HS n=6, LS n=8). Representative SR-stained sections and segmentation results are shown (a, right and lower panels). Positive areas were also quantified from segmentation images for Masson's trichrome (MT) (b), *Wisteria floribunda* agglutinin (WFA) (c), and *Maackia amurensis* hemagglutinin (MAH) (d). The degree of positive areas was summarized for each high-salt (HS) and low-salt (LS) rat using representative samples (n=3 each) (e).

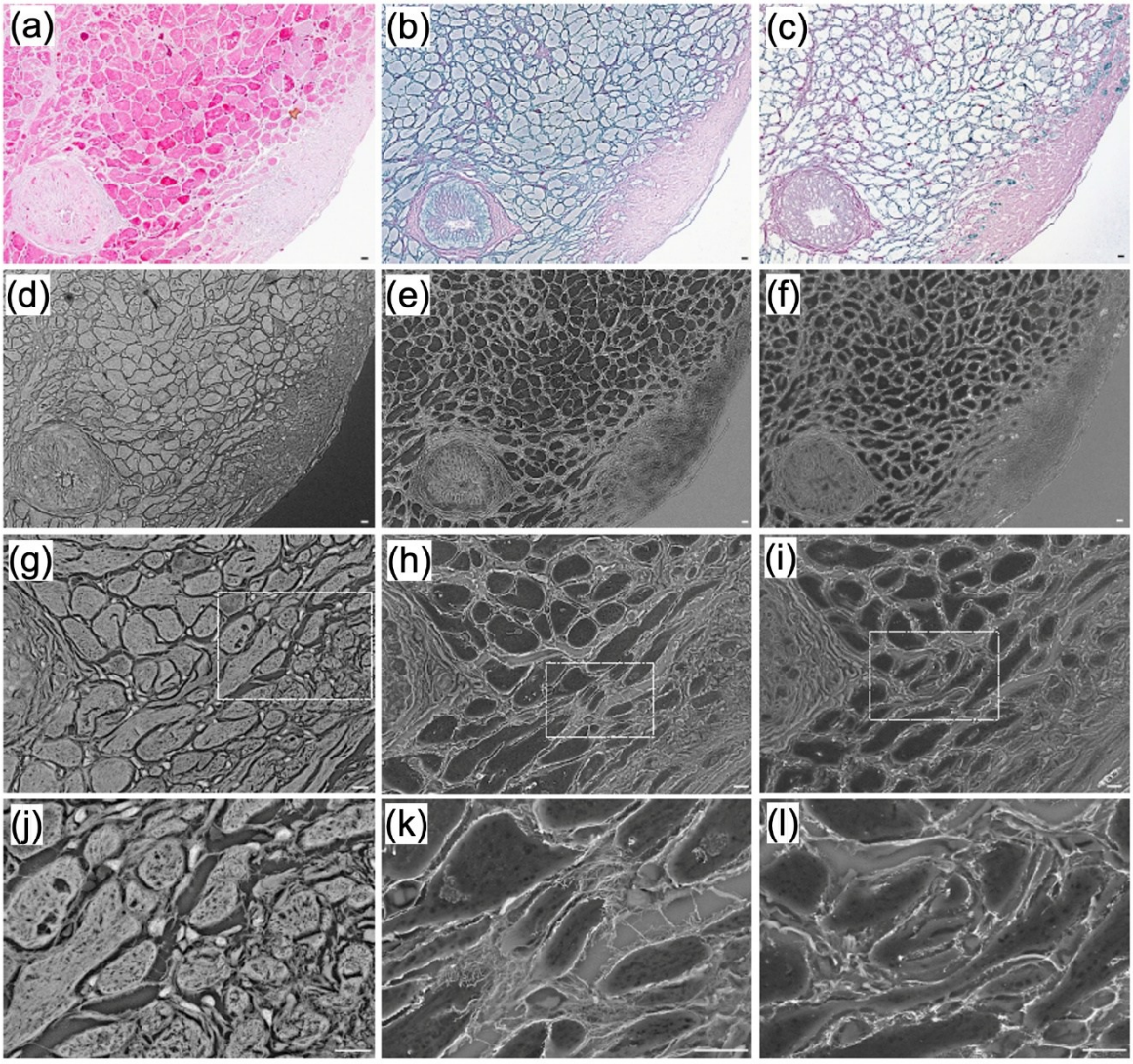

Supplementary Fig. 4 The comparison of staining methods for low-vacuum scanning electron microscopy (LVSEM). Serial sections were stained with Masson's phosphotungstic acid (Masson's PTA) (a, d, g, and j), Reticulin stain (b, e, h, and k), and modified periodic acid-methenamine silver (PAM) (c, f, i, and l). (a–c) Bright-field image. (d–f) LVSEM images of the same field of view as a–c, respectively. (g–i) Magnified images of d–f, respectively. (j–l) Magnified images of g–i. Scale bars: 10 μm.

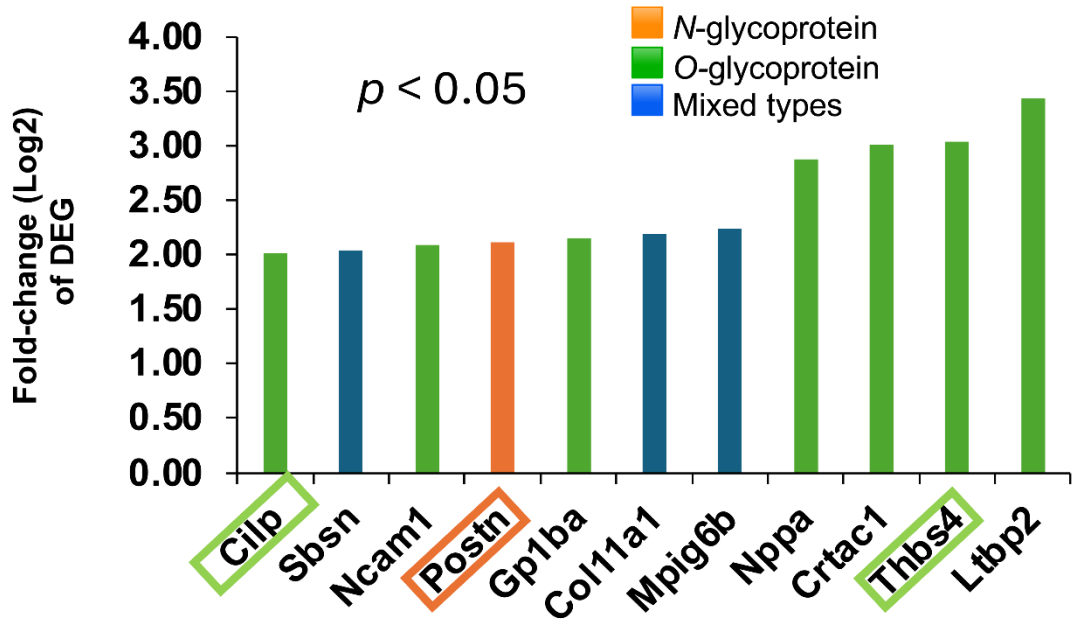

Supplementary Fig. 5 Differential gene expression (DEG) analysis of candidate *N*- and *O*-glycoproteins. The graph shows 11 genes significantly differentially expressed in HS vs. LS hearts (Log2 fold change > 2, $P < 0.05$). These genes met the selection criteria of encoding secreted or extracellular matrix proteins with predicted possible *N*- and *O*-glycosylation sites. The *N*-glycoprotein (Postn) and *O*-glycoproteins (Cilp and Thbs4) selected in this study are highlighted in orange and green, respectively.

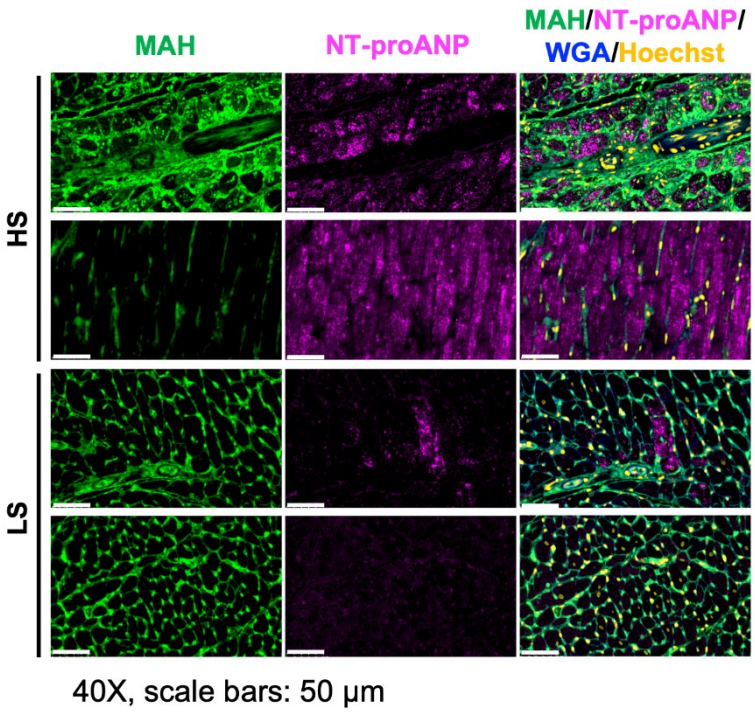

Supplementary Fig. 6 Co-staining of *Maackia amurensis* hemagglutinin (MAH) and candidate *O*-glycoprotein NPPA (N-terminal pro-atrial natriuretic peptide; NT-proANP), in *Wisteria floribunda* agglutinin $(WFA)^{+}$ and WFA^{-} regions of high-salt-treated (HS) and low-salt-treated (LS) rat hearts. Wheat germ agglutinin (WGA) and Hoechst were used to visualize the membranes and nuclei, respectively.